CRCLEME
Cooperative Research Centre for
Landscape Evolution & Mineral Exploration

OPEN FILE REPORT SERIES

CSIRO
EXPLORATION AND MINING

AMIRA
Australian Mineral Industries Research Association Limited ACN 004 448 266

# THE MINERALOGICAL AND GEOCHEMICAL EFFECTS OF WEATHERING ON SHALES AT THE PANGLO DEPOSIT, EASTERN GOLDFIELDS, WESTERN AUSTRALIA

*K.M. Scott and L.E. Dotter*

**CRC LEME OPEN FILE REPORT 48**

September 1998

(CSIRO Division of Exploration Geoscience Report 171R, 1990.
Second impression 1998)

CRC LEME is an unincorporated joint venture between The Australian National University, University of Canberra, Australian Geological Survey Organisation and CSIRO Exploration and Mining, established and supported under the Australian Government's Cooperative Research Centres Program.

Australian Mineral Industries Research Association Limited ACN 004 448 266

CRCLEME
Cooperative Research Centre for Landscape Evolution & Mineral Exploration

CSIRO
EXPLORATION AND MINING

# THE MINERALOGICAL AND GEOCHEMICAL EFFECTS OF WEATHERING ON SHALES AT THE PANGLO DEPOSIT, EASTERN GOLDFIELDS, WA

*K.M. Scott and L.E. Dotter*

**CRC LEME OPEN FILE REPORT 48**

September 1998

(CSIRO Division of Exploration Geoscience Report 171R, 1990.
Second impression 1998)



CRC LEME is an unincorporated joint venture between The Australian National University, University of Canberra, Australian Geological Survey Organisation and CSIRO Exploration and Mining
*Headquarters:* CRC LEME c/o CSIRO Exploration and Mining, Private Bag, PO Wembley, Western Australia, 6014

## RESEARCH ARISING FROM CSIRO/AMIRA REGOLITH GEOCHEMISTRY PROJECTS 1987-1993

In 1987, CSIRO commenced a series of multi-client research projects in regolith geology and geochemistry which were sponsored by companies in the Australian mining industry, through the Australian Mineral Industries Research Association Limited (AMIRA). The initial research program, "Exploration for concealed gold deposits, Yilgarn Block, Western Australia" (1987-1993) had the aim of developing improved geological, geochemical and geophysical methods for mineral exploration that would facilitate the location of blind, buried or deeply weathered gold deposits. The program included the following projects:

**P240: Laterite geochemistry for detecting concealed mineral deposits (1987-1991).** Leader: Dr R.E. Smith.
Its scope was development of methods for sampling and interpretation of multi-element laterite geochemistry data and application of multi-element techniques to gold and polymetallic mineral exploration in weathered terrain. The project emphasised viewing laterite geochemical dispersion patterns in their regolith-landform context at local and district scales. It was supported by 30 companies.

**P241: Gold and associated elements in the regolith - dispersion processes and implications for exploration (1987-1991).** Leader: Dr C.R.M. Butt.
The project investigated the distribution of ore and indicator elements in the regolith. It included studies of the mineralogical and geochemical characteristics of weathered ore deposits and wall rocks, and the chemical controls on element dispersion and concentration during regolith evolution. This was to increase the effectiveness of geochemical exploration in weathered terrain through improved understanding of weathering processes. It was supported by 26 companies.

These projects represented "an opportunity for the mineral industry to participate in a multi-disciplinary program of geoscience research aimed at developing new geological, geochemical and geophysical methods for exploration in deeply weathered Archaean terrains". This initiative recognised the unique opportunities, created by exploration and open-cut mining, to conduct detailed studies of the weathered zone, with particular emphasis on the near-surface expression of gold mineralisation. The skills of existing and specially recruited research staff from the Floreat Park and North Ryde laboratories (of the then Divisions of Minerals and Geochemistry, and Mineral Physics and Mineralogy, subsequently Exploration Geoscience and later Exploration and Mining) were integrated to form a task force with expertise in geology, mineralogy, geochemistry and geophysics. Several staff participated in more than one project. Following completion of the original projects, two continuation projects were developed.

**P240A: Geochemical exploration in complex lateritic environments of the Yilgarn Craton, Western Australia (1991-1993).** Leaders: Drs R.E. Smith and R.R. Anand.
The approach of viewing geochemical dispersion within a well-controlled and well-understood regolith-landform and bedrock framework at detailed and district scales continued. In this extension, focus was particularly on areas of transported cover and on more complex lateritic environments typified by the Kalgoorlie regional study. This was supported by 17 companies.

**P241A: Gold and associated elements in the regolith - dispersion processes and implications for exploration.** Leader: Dr. C.R.M. Butt.
The significance of gold mobilisation under present-day conditions, particularly the important relationship with pedogenic carbonate, was investigated further. In addition, attention was focussed on the recognition of primary lithologies from their weathered equivalents. This project was supported by 14 companies.

Although the confidentiality periods of the research reports have expired, the last in December 1994, they have not been made public until now. Publishing the reports through the CRC LEME Report Series is seen as an appropriate means of doing this. By making available the results of the research and the authors' interpretations, it is hoped that the reports will provide source data for future research and be useful for teaching. CRC LEME acknowledges the Australian Mineral Industries Research Association and CSIRO Division of Exploration and Mining for authorisation to publish these reports. It is intended that publication of the reports will be a substantial additional factor in transferring technology to aid the Australian Mineral Industry.

This report (CRC LEME Open File Report 48) is a Second impression (second printing) of CSIRO, Division of Exploration Geoscience Restricted Report 171R, first issued in 1990, which formed part of the CSIRO/AMIRA Project P241.

**Copies of this publication can be obtained from:**
The Publication Officer, c/- CRC LEME, CSIRO Exploration and Mining, PMB, Wembley, WA 6014, Australia. Information on other publications in this series may be obtained from the above or from http://leme.anu.edu.au/
**Cataloguing-in-Publication:**
Scott, K.M.
The mineralogical and geochemical effects of weathering on shales at the Panglo Deposit, Eastern Goldfields, WA
ISBN 0 642 28217 X
1. Mineralogy 2. Weathering 3. Shale - Western Australia 4. Geochemistry.
I. Dotter, L.E. II. Title
CRC LEME Open File Report 48.
ISSN 1329-4768

## TABLE OF CONTENTS



## LIST OF TABLES

## LIST OF FIGURES

## SUMMARY

Examination of phyllosilicates, oxide phases, alunite and, where present, sulfides and carbonates in 10 samples of fresh and weathered shale from the Panglo area has helped elucidate how elements are retained during weathering. Chalcophile elements are strongly retained by Fe oxides and Sr and Ba (plus As and Cu) are retained by alunite. Micas, which are essentially unaffected by weathering, appear to have low Na and Fe contents in mineralized profiles and higher contents elsewhere.

By comparing mineralized and barren shale profiles, Fe and chalcophile elements (As, Mo, Sb and W) appear to be enriched and Na, Ba and Sr depleted in weathered shales above secondary gold mineralization at Panglo.

## 1. INTRODUCTION

In a previous report Scott (1989a) has shown that shale profiles along Section 4200N have more extensive development of alunite and less paragonite above mineralization than in barren shale profiles. The mineralized profile also tends to have higher Fe, As, Cr, Sc and W but lower Sr than the barren profile. However the barren profile, being located only ~40 m from mineralization, does contain sub-economic gold. Thus shale profiles well to the north of the Panglo mineralization (Section 6500N; Fig. 1) have been studied in an attempt to better define background characteristics of shales affected by weathering.

Results from these northern shale profiles and analyses of fresh shales (obtained from diamond drilling) are compared to results from shale profiles on Section 4200N to define better the changes which occur during weathering of shales at Panglo. Thus this report complements that on the weathering effects on mafic and ultramafic rocks at Panglo (Scott, 1990a).

## 2. SAMPLES AND METHODS

Reverse circulation holes PSRC 171 and 172 were drilled 40m apart along Section 6500N i.e. almost 2km N of the Panglo mineralization (Figs. 1 and 2). Both holes were drilled at 60°E and depths throughout this report are actually distances along these drill holes unless otherwise indicated. The samples studied were 1 metre composites from the drilling (samples between 0 and 4 m from PSRC 171 however could not be found).

Six samples of black carbonaceous to grey dolomitic shale from deep diamond drilling (PSRCD 309 and PSRCD 310) into fresh shale in the deposit area have also been analysed.

Mineralogical and chemical analytical methods (including electron microprobe methods) are as described by Scott (1989b) and Ramsden and French (1990). The Au contents of reverse circulation composites were determined by Pancontinental Mining Ltd. during the course of exploration. Four samples of unweathered shale had their Au content determined by Neutron Activation Analysis by Becquerel Laboratories, Lucas Heights.

## 3. RESULTS

### 3.1 PSRC 171 - a barren hole

The mineralogy down this hole from 4 to 60m is shown in Fig. 3. It is characterized by the presence of quartz, kaolinite, mica, Fe oxides and halite throughout. However the interval 4-16m is identified as the hematite/alunite/paragonite zone. It is white to pale brown in colour with hematite in the uppermost portion and hematite and goethite below 8 m. The underlying goethite/alunite/paragonite zone (16-26 m) is similar in colour but contains only goethite (without hematite) and some smectitic clay. Between 26 and 39 m the goethite/paragonite zone is more white to grey in colour and does not contain the alunite of the zones above. Deeper material from 39-60 m (goethite zone) is more yellow in colour due to its increased goethite content and paragonite is not present (Fig. 3). Quartz veins are present in this interval (Fig. 2).

Chemical analyses reveal a progressive decrease in Si and Sr down the profile (Tables 1 and 2). The hematite/alunite/paragonite zone also tends to be slightly enriched in Fe and B, with S also significant. Arsenic contents are however quite low. The goethite/alunite/paragonite zone also has high S contents but low Fe, Mg and As contents. Goethite/paragonite and goethite zones have lower S than the zones above but As, Ni and W tend to be higher in these two zones. K, B and Cr are lowest and Pb highest in the goethite zone (Table 2).

3.2 PSRC 172 - a mineralized hole

The minerals present in this hole from 0 to 60m are similar to those in PSRC 171. However their abundances vary with paragonite only intermittently developed in PSRC 172 and goethite and hematite more abundant in PSRC 172, especially above 27 m (cf. Figs. 3 and 4).

The interval 0-18 m (goethite/alunite zone) is brown and grey in colour and is relatively goethite rich. Paragonite is only present in one sample at the base of this zone (Fig. 4). Quartz veining is present throughout this zone (Fig. 2). In the interval between 18 and 27 m hematite is strongly developed in addition to goethite. Quartz veining is also present but alunite is not. This hematite/goethite zone is brown and grey in colour. The interval 27-43m is more pale in colour (grey-white) due to its lesser Fe oxide content than above but other mineralogical abundances are not significantly different. The basal paragonite zone (43-60 m) is also grey-white in colour but some black (fresher) material occurs at the base of this zone, where minor chlorite and moderate amounts of paragonite occur (Fig. 4).

Despite the presence of quartz veining in the interval above 27m, $SiO_2$ contents appear lower there than deeper in the profile due to dilution by the abundant Fe oxides in the upper part of the profile (Tables 3 and 4). The goethite/alunite zone is characterized by high Fe, S, As, Cu, Ni, Pb, V, W and Zn contents. Au appears to be enriched in the uppermost 6 m but mainly due to one highly anomalous sample (29635; Table 3). Fe and associated As, Ni and Zn contents are greater in the hematite/goethite zone than in the goethite/alunite zone, but Si, K and Ba are low in this Fe-rich zone. The Fe-poor zone has concentrations of most elements, intermediate between the Fe rich zones above and the underlying slightly fresher material of the paragonite zone which is characterized by high Na and Sr but low Cr, Sc and V (Table 4).

### 3.3. Unweathered Shales

The six samples of unweathered shale from DDHs PSRCD 309 and PSRCD 310 are both mineralized and unmineralized. The mineralized samples (105681 and 105682) consist of quartz, muscovite, chlorite, pyrite, ± dolomite and siderite. Unmineralized samples (108074-76 and 105683) contain all these minerals plus albite ± smectitic clay ± talc ± apatite although calcite may be present in place of dolomite and siderite in some cases.

Although there are some chemical variations due to variable carbonate development (both compositions and abundance), the mineralized shale contains higher Si, Fe, S, Ag, Au, B, Co, Cu, Mo, Ni, Pb, Sb, Sn and W contents. Al, Ti, P, Ga, Sr, Tl, V, Zn and Zr are however lower than in the barren shale (Table 5). The enriched elements are essentially the chalcophile elements although Tl and Zn might have been expected in that group too (see discussion). Arsenic contents in all these samples are quite low (Table 5).

### 3.4. Electron microprobe studies of shale-hosted minerals

The white micas (muscovite, paragonite, illite and brammallite) have generally low abundances of trace elements except for Ba and Sr, the latter only being significant when the Na content of the white mica is greater than 0.36 mol (Table 6). Na contents are low (<0.36 mol) in the white micas from mineralized profiles in PSRC 341 and PSRC 172 and in the fresh material below mineralization i.e. from PSRCD 309 and PSRCD 310 (Fig. 5). These samples with the exception of one of the micas from PSRC 172 and one of the fresh samples also tend to have lower Fe* ratios (i.e. Fe/(Fe + Mg + Mn)) than micas from unmineralized profiles. High Cl contents relative to F occur in most of the Na-rich micas from the barren profile, PSRC 340 (Table 6).

Of the other phyllosilicates, chlorite is only present in unweathered samples. It has relatively low trace element contents except for Zn (>300 ppm). Cr and Ni, which are high in ultramafic rocks, are quite low. Kaolinite may have significant Cr and Ba contents - the latter, as implied by its relationship to K, reflecting illite contamination/intergrowth in the kaolinite (Table 7).

Tourmaline (dravite) bears a significant Cr content (Table 7).

Albite from unweathered shale in PSRCD 309 contains < 1% (An + Or). It also contains 340 ppm Sr, but its Ba content is <100 ppm.

Goethite may contain up to 2000 ppm Cr, 610 ppm Ni, 950 ppm Cu, 1900 ppm Zn, 1.99% As and 190 ppm Sb. Hematite, from more limited data, appears to contain lower levels of these elements (Table 8). Thus goethite is usually the major host for chalcophile elements in weathered material.

Rutiles and ilmenite have up to 1600 ppm Cr (Table 8) - levels similar to those in these minerals in mafic volcanics but well less than those in ultramafic rocks (Scott, 1990a).

Both dolomite and calcian siderite occur in fresh samples of shale. The earlier generation of dolomite is more ferroan than later dolomite in sample 105682 (Table 9). Mn contents are also quite significant in the dolomites and siderites. Traces of Sr (up to 200 ppm) may be present in dolomite but not siderite.

Alunite has the general formula K $Al_3$ $(SO_4)_2$ $(OH)_6$ but that in weathered shales at Panglo contain 0.15 to 0.36 mol of Na in K sites and minor Fe and minor to trace Cu in the Al sites. Trace $AsO_4$ and significant $PO_4$ may also occur in the $SO_4$ sites (Table 10). The alunite from above Au-mineralization contains less Na, Sr and Ba than alunite from barren profiles. However the Sr content of alunite from the As-rich profile through PSRC 172 is similar to that in the Au-mineralized profile, PSRC 341 (Table 10).

Pyrite in the fresh samples below secondary mineralization contain variable Co, Cu and Ni contents, but As and Zn are uniformly low (Table 11). Although on the basis of size and composition, several generations of pyrite appear to be present in these two samples, because of the small number of analyses, no detailed paragenesis can be established. Sphalerite from sample 108074 contains 7 mol% FeS.

# 4. DISCUSSION

## 4.1 Evaluation of weathered shale profiles

PSRC 171 provides a good background profile for shales of the Panglo area. Comparison of PSRC 171 with the mineralized profile, PSRC 342, suggests that Fe, K, As, Mo, W and Zn are enriched in the profile above secondary Au mineralization with Ag, Co and Sn also enriched in the mineralized zone and for 10m above. Na, Ba and Sr are depleted in the mineralized hole relative to the barren hole (cf. Tables 2 and 12). These differences between a well mineralized profile and completely barren profile confirm the findings of Scott (1989a), derived by comparing well-mineralized and poorly mineralized profiles (PSRC 342 and PSRC 340, respectively).

PSRC 172 differs from the PSRC 171 by having more abundant goethite but less abundant paragonite and alunite in its upper part (Figs. 2 and 3). Thus Fe contents are greater and Na contents lower in PSRC 172 (Tables 2 and 3). Siderophile and chalcophile elements, especially As, Co, Cr, Ni, Pb and Zn are also associated with the Fe in PSRC 172 (Table 3). Furthermore Sr is depleted relative to PSRC 171 (Tables 2 and 4). Thus this profile appears to have many of the characteristics of the mineralized profile (PSRC 342; Table 12). However the alunite abundance in PSRC 172 is quite low, even relative to the barren profile, PSRC 171 (cf. Figs 3 and 4). Therefore PSRC 172 is distinguished from the mineralized hole PSRC 342 by its low alunite content and the lack of secondary Au at a vertical depth of 40 m (Scott, 1989a). However some significant Au does occur associated with extensive quartz veining higher in the profile in PSRC 172 (Fig. 2; Section 3.2). Because As is intimately associated with Au and the quartz veins above 27m, it is assumed that this Au is essentially in situ (see also below) i.e. this hole is mineralized but not with secondary Au at ~40 m vertical depth.

## 4.2 Mineralogical features of shale profiles

White micas have Na <0.36 mol and generally Fe* <0.4 when present in fresh shales from beneath mineralization or within weathered but mineralized shale profiles as in PSRC 341 and PSRC 172. These features allow a line A-B to be drawn to separate the fields of micas from mineralized and unmineralized profiles (Fig. 5). However, because Na-rich micas also tend to be enriched in Cl and Sr (Table 6), it is possible that the saline groundwaters (which occur in the weathered profile at Panglo) have reacted with the micas to enrich them in Na, Cl and Sr during post-Tertiary times, as suggested in an earlier report (Scott and Dickson, 1989). Closer inspection of the data reveals that the Na-, Cl- and Sr-enriched micas are almost exclusively those from the barren profile PSRC 340 (Table 6). Because the micas from barren profiles are unlikely to be more susceptible to alteration by saline solutions than those from mineralized profiles, mica compositions are considered to be essentially those derived during the primary mineralization event and to have remained relatively stable during subsequent later lateritic and arid weathering events at Panglo. Where the original muscovite or paragonite is altered to an illitic composition during weathering whether illite or brammallite forms depends upon whether the parental mica was K- or Na-rich (e.g. Table 6). Thus mica compositions offer potential as an indicator of mineralization, as previously suggested at Mt Magnet (Scott, 1990b).

Chlorite is unstable during weathering of shales and hence its substantial Zn content (Table 7) is dispersed during weathering processes. Fe* ratios of chlorites do not reflect those of co-existing micas unlike the case at Mt Magnet (Scott, 1990b).

Kaolinite generally has low chalcophile element contents but Cr and Ba contents may be significant (Table 7). Ba contents in the kaolinite correlate with K content and probably reflect the presence of admixed micaceous phases. Intergrown Fe oxides are also often present in kaolinite and responsible for the high Fe* ratios recorded in Table 7.

The Fe oxides, goethite and hematite provide hosts for siderophile (Cr) and chalcophile elements (Ni, Cu, Zn, As, Sb) which may be freed during the breakdown of silicates and sulfides during weathering. Rutile and, perhaps ilmenite, remain stable during weathering processes and hence their contained Cr is kept immobile during weathering. The Cr within these Ti-phases is similar to that in similar phases in mafic volcanics at Panglo (Scott, 1990a).

Alunite may contain substantial amounts of the chalcophile elements Cu and As (0.01 mol ≃ 1000 ppm Cu or As). However the most significant feature is the higher Sr and Ba contents in the alunite in drill hole PSRC 340 relative to that in the more mineralized drill holes PSRC 172 and PSRC 341 (Table 10). Together with the Sr in the micas in barren profiles, alunite thus appears to explain the high Sr lateral to mineralization (Scott, 1989a; Scott and Dickson, 1989). However, whereas mica is essentially unaffected by weathering processes, alunite is formed by them. In fact the significant Na content of the alunites (0.15-0.36 mol, Table 10) suggests that the alunites may be in equilibrium with the current Na-rich groundwaters at Panglo (cf. Parker, 1962). Thus if the Sr within the micas was always there (as argued above) that in the alunites has been derived during weathering. The most likely sources are carbonates and feldspars which may contain several hundred ppm Sr at Panglo (Section 3.4). Because Sr contents are generally higher in calcite than in dolomite ~~and~~ siderite (due to its greater abundance of Ca) more Sr might thus be released during weathering of barren profiles (where calcite and dolomite occur) than during weathering of mineralized profiles where dolomite and siderite occur (Section 3.3).

Carbonate and pyrite data is restricted to two samples (Tables 9 and 11). However, because of the relationship between these two types of minerals (e.g. Fig. 6), even this small amount of data suggests that their compositions may be useful in exploration. Indeed features like the Fe and Mn contents of the various carbonate minerals can reflect proximity to mineralization in the Yilgarn Block (e.g. Neal and Phillips, 1987; Scott, 1990a).

Results also suggest that carbonate and pyrite compositions have varied with time (e.g. Figs. 7 and 8). However, because of the susceptibility of these minerals to weathering such applications can only be made with unweathered material. With weathering of the carbonates, the freed Ca and Mg are generally lost but Fe, Mn and any Ba and Sr from the carbonates are at least partially retained as oxides and in alunite. The chalcophile elements freed when pyrite weathers are substantially retained by incorporation into/adsorption onto Fe oxides (Table 8).

### 4.3 Relevance to exploration in shale sequences

Features of mineralized and barren shale profiles are summarized in Figs. 9 and 10. These show the greater development of paragonite in the barren profile and the greater K and Fe contents in the mineralized profile. Soils above shales at Panglo are usually thin and have a large introduced/transported component within them, reflected by the presence of minerals (plagioclase, calcite, chlorite and talc) which are not found in underlying leached saprolite (Figs 9 and 10; Scott and Dickson 1989). Thus the Au contents of such soils do not give a good indication of underlying Au mineralization.

The Cr content of such soils may not be significantly different from those over volcanics. However the much lower Cr contents of weathered shales than weathered volcanics clearly distinguishes the two major rock types at Panglo (cf. Fig. 9 and 10; Scott, 1990a).

The composition of the micas from mineralized drill holes (PSRC 172 and PSRC 341) and the fresh shales are characterized by low Na contents and often low Fe contents (Fig. 5). (Note however that in highly weathered material, Fe* ratios may be influenced by intergrown Fe oxides). These features of micas are as found in the volcanic rocks at Panglo (Scott, 1990a). The association of K-enrichment with Au, As and quartz-veining in the upper 27 m of PSRC 172 also suggests that the K enrichment is closely associated with Au and pyrite in quartz veins prior to weathering. In PSRC 172, the effect of weathering has been destruction of pyrite and mobilization of primary Au (probably Ag-bearing, by comparison with other primary Au in the region e.g. Robertson et al., 1988) and its reprecipitation as pure secondary Au nearby. It is also possible that such Au has been armoured against weathering by the quartz and has not moved at all. (Unfortunately no suitable samples to examine the Au were available). Nevertheless this study seems to confirm the suggestion that K-enrichment of the rocks, developed during mineralization processes, is preserved during weathering (Scott, 1990a).

If this paragenesis is substantially correct the high level occurrence of As and quartz-veining in PSRC 172 represents Au mineralization which has not been mobilized very far and is thus perched well above the level where secondary mineralization is generally encountered at Panglo. Similar perched Au concentrations occur associated with quartz veining in PSRC 312 along Section 4200N (R.W. Howard, pers. comm. 1988). The presence of such occurrences may also suggest that most of the secondary Au mineralization which occurs at 40m depth is derived from deep in the weathering profile i.e. not by downward movement from high level occurrences. Therefore As, W, Mo and Sb should be considered reliable pathfinders for Au in weathered shales even though this study reveals that the Au so indicated may not necessarily be the higher grade supergene variety being sought in the Panglo area.

## 5. CONCLUSIONS

Of the minerals (mica, chlorite, albite, pyrite, carbonates and rutile) present in fresh shales at Panglo, only mica and rutile are relatively resistant to weathering. The destruction of the other minerals frees elements like Ca, Mg and Na to be widely dispersed but Fe and Mn form oxide phases which are responsible for retaining many chalcophile elements e.g. As, Sb, Cu. The formation of alunite as a breakdown product of pyrite also results in the stabilization of normally mobile Sr as well as Ba and some chalcophile elements (especially Cu and As).

Because of the stability of micas, some of their compositional features like low Na and Fe contents in weathered mineralized profiles may be useful as pathfinders to mineralization at Panglo.

With the completely barren profile provided by study of PSRC 171, mineralized shale profiles are verified as being enriched in Fe and chalcophile elements (As, W, Mo and Sb) and depleted in Na, Ba and Sr relative to barren shale profiles (Scott, 1989a).

The presence of high Fe and As contents in the upper part of PSRC 172 is considered to reflect high level quartz- and pyrite-associated Au mineralization in that hole.

## 6. ACKNOWLEDGEMENTS

The management of the Exploration Division of Pancontinental Mining Ltd. is thanked for a willingness to provide samples, results and plans of the Panglo deposit. In particular the assistance of, and discussions with, Bob Howard are acknowledged. Members of the project 241 team are also thanked for valuable discussions.

X-ray diffractograms were run by A.R. Horne. Assistance with electron microprobe determinations was given by D.H. French and K.M. Kinealy. H.R. Han, K. Bone, H. Orban and A. Martinez helped by performing chemical analyses. Diagrams have been prepared with the assistance of I.D.M. Robertson, A. Sheehan and B.L. Dickson (CSIRO Institute of Minerals, Energy and Construction).

## 7. REFERENCES

Parker, R.L., 1962. Isomorphous substitution in natural and synthetic alunite. Am. Mineralogist 47: 128-136.

Neall, F.B. and Phillips, G.N., 1987. Fluid-wall rock interaction in an Archean hydrothermal gold deposit: a thermodynamic model for the Hunt Mine, Kambalda. Econ. Geol. 82: 1679-1694.

Ramsden, A.R. and French, D.H., 1990. Routine trace-element capabilities of electron microprobe analysis in mineralogical investigations: an empirical evaluation of performance using spectrochemical standard glasses. Can. Mineralogist 28: 171-180.

Robertson, I.G., Jones, D.A., Smith, B.E. and Bloch, J., 1988. The Paddington Gold mine in Bicentential Gold 88 Excursion No. 6 Guide, Part III: Norseman-Wiluna Belt. pp 91-99.

Scott, K.M., 1989a. Mineralogy and geochemistry of weathered shale profiles at the Panglo Gold Deposit, Eastern Goldfields, W.A. (AMIRA P241: Weathering Processes) CSIRO Div. of Exploration Geoscience Restricted Report 32R.

Scott, K.M., 1989b. Mineralogy and geochemistry of weathered mafic/ultramafic volcanics from Section 4200N at Panglo, Eastern Goldfields, W.A. (AMIRA P241: Weathering Processes). CSIRO Div. of Exploration Geoscience Restricted Report 42R.

Scott, K.M., 1990a. The mineralogical and geochemical effects of weathering on volcanics from the Panglo Deposit, Eastern Goldfields, W.A. (AMIRA P241: Weathering Processes). CSIRO Div. of Exploration Geoscience Restricted Report 143R.

Scott, K.M., 1990b. Electron microprobe studies of minerals from weathered profiles, Parkinson Pit and environs, Mt Magnet, W.A. (AMIRA P241: Weathering Processes) CSIRO Div. of Exploration Geoscience Restricted Report 147R.

Scott, K.M. and Dickson, B.L., 1989. Radioelements in weathered shales and mafic voclanics, Panglo Gold Deposit, Eastern Goldfields, W.A. (AMIRA P241: Weathering Processes/AMIRA P263: Airborne Gamma Ray Surveys) CSIRO Div. of Exploration Geoscience Restricted Report 41R.

Table 1. Chemical composition of samples, barren hole, PSRC 171
(majors, wt%; minors, ppm)

| Sample No. | 29571 | 29575 | 29583 | 29587 | 29593 | 29599 | 29607 | 29611 | 29623 | 29629 |
|---|---|---|---|---|---|---|---|---|---|---|
| Depth (m) | 4-5 | 8-9 | 15-16 | 19-20 | 25-26 | 31-32 | 38-39 | 42-43 | 54-55 | 59-60 |
| $SiO_2$ | 75.2 | 66.7 | 63.5 | 67.3 | 67.6 | 65.7 | 63.0 | 67.8 | 61.6 | 59.3 |
| $Al_2O_3$ | 14.8 | 16.5 | 18.9 | 17.9 | 20.2 | 17.4 | 19.8 | 19.7 | 20.0 | 22.5 |
| $Fe_2O_3$ | 2.50 | 1.63 | 1.36 | 0.80 | 0.86 | 2.51 | 0.97 | 1.23 | 2.30 | 0.86 |
| MgO | 0.28 | 0.54 | 0.51 | 0.29 | 0.25 | 0.36 | 0.52 | 0.27 | 0.49 | 0.60 |
| CaO | <0.04 | 0.09 | 0.04 | <0.04 | <0.04 | <0.04 | 0.09 | <0.04 | <0.04 | <0.04 |
| $Na_2O$ | 1.13 | 3.42 | 3.07 | 2.13 | 1.37 | 2.87 | 2.57 | 1.12 | 2.66 | 2.78 |
| $K_2O$ | 3.02 | 2.12 | 2.51 | 2.06 | 2.60 | 2.27 | 2.88 | 1.95 | 1.41 | 1.31 |
| $TiO_2$ | 0.53 | 0.47 | 0.52 | 0.50 | 0.58 | 0.51 | 0.57 | 0.38 | 0.48 | 0.66 |
| $SO_3$ | 0.05 | 0.44 | 1.07 | 1.20 | 0.27 | 0.21 | 0.19 | 0.07 | 0.22 | 0.17 |
| Ag | <0.1 | <0.1 | <0.1 | <0.1 | <0.1 | <0.1 | 0.2 | <0.1 | <0.1 | 0.2 |
| As | 79 | 21 | 31 | 28 | 48 | 66 | 140 | 110 | 790 | 180 |
| Au | <0.02 | <0.02 | 0.04 | <0.02 | <0.02 | <0.02 | <0.02 | <0.02 | <0.02 | <0.02 |
| B | 80 | 70 | 100 | 40 | 90 | 50 | 80 | 40 | 30 | 40 |
| Ba | 830 | 260 | 700 | 570 | 660 | 600 | 840 | 730 | 590 | 550 |
| Co | <5 | <5 | <5 | <5 | <5 | 8 | <5 | 5 | 6 | 8 |
| Cr | 200 | 220 | 260 | 160 | 250 | 210 | 240 | 68 | 170 | 160 |
| Cu | <5 | 6 | 6 | <5 | 9 | 28 | 14 | 17 | 26 | 16 |
| Ga | 30 | 20 | 20 | 20 | 30 | 20 | 30 | 30 | 20 | 30 |
| Ge | 1 | 0.3 | 0.5 | 0.3 | 0.3 | 0.3 | 0.1 | 0.1 | 0.1 | 0.3 |
| Mo | 3 | 3 | 5 | 1 | 2 | 3 | 3 | 1 | 2 | 2 |
| Ni | 20 | 28 | 46 | 22 | 35 | 83 | 37 | 52 | 52 | 50 |
| Pb | <50 | <50 | <50 | <50 | <50 | 55 | <50 | <50 | 95 | 67 |
| Sc | <5 | 11 | 15 | 13 | 6 | <5 | <5 | 6 | 11 | 7 |
| Sn | 2 | 1 | 2 | 1 | 2 | 2 | 2 | 1 | 3 | 4 |
| Sr | 190 | 210 | 240 | 180 | 180 | 120 | 110 | 64 | 46 | 33 |
| V | 110 | 84 | 96 | 68 | 96 | 91 | 98 | 54 | 88 | 97 |
| W | <10 | <10 | <10 | <10 | <10 | <10 | 20 | 15 | 30 | 40 |
| Y | 7 | 7 | 7 | 7 | 8 | 9 | 8 | 7 | 10 | 21 |
| Zn | <5 | <5 | <5 | <5 | <5 | 5 | <5 | <5 | 14 | 10 |
| Zr | 200 | 140 | 170 | 190 | 200 | 190 | 190 | 180 | 190 | 340 |
| Ti/Zr | 16 | 19 | 18 | 16 | 18 | 17 | 18 | 13 | 16 | 12 |

Note: $P_2O_5$ < 0.1, MnO <0.04%; Sb < 10 ppm

Table 2 Average compositions for zones, PSRC 171 (Barren) (major elements, wt%; minors, ppm)

| Zone<br>Depth (m)<br>No. of<br>Samples | Hem/al/parag<br>4-16<br><br>3 | Goe/al/parag<br>16-26<br><br>2 | Goe/parag<br>26-39<br><br>2 | Goe<br>39-60<br><br>3 |
|---|---|---|---|---|
| $SiO_2$ | 68.5 | 67.5 | 64.4 | 62.9 |
| $Al_2O_3$ | 16.7 | 19.1 | 18.6 | 20.7 |
| $Fe_2O_3$ | 1.83 | 0.83 | 1.74 | 1.46 |
| MgO | 0.44 | 0.27 | 0.44 | 0.45 |
| CaO | 0.05 | <0.04 | 0.06 | <0.04 |
| $Na_2O$ | 2.54 | 1.75 | 2.72 | 2.19 |
| $K_2O$ | 2.55 | 2.33 | 2.58 | 1.56 |
| $TiO_2$ | 0.51 | 0.54 | 0.54 | 0.51 |
| $SO_3$ | 0.52 | 0.74 | 0.20 | 0.15 |
| Ag | <0.1 | <0.1 | 0.1 | 0.1 |
| As | 44 | 38 | 100 | 360 |
| Au | 0.02 | <0.02 | <0.02 | <0.02 |
| B | 83 | 65 | 65 | 40 |
| Ba | 600 | 620 | 720 | 620 |
| Co | <5 | <5 | 5 | 6 |
| Cr | 230 | 210 | 230 | 130 |
| Cu | 5 | 6 | 21 | 20 |
| Ga | 23 | 25 | 25 | 27 |
| Ge | 0.6 | 0.3 | 0.2 | 0.2 |
| Mo | 4 | 2 | 3 | 2 |
| Ni | 31 | 29 | 60 | 51 |
| Pb | <50 | <50 | <50 | 62 |
| Sc | 10 | 10 | <5 | 8 |
| Sn | 2 | 2 | 2 | 3 |
| Sr | 210 | 180 | 120 | 48 |
| V | 97 | 82 | 95 | 80 |
| W | <10 | <10 | 13 | 28 |
| Y | 7 | 8 | 9 | 13 |
| Zn | <5 | <5 | <5 | 9 |
| Zr | 170 | 200 | 190 | 240 |

Note: $P_2O_5$ <0.1, MnO < 0.04%

Table 3. Chemical composition of samples, mineralized hole, PSRC 172
(majors, wt%; minors, ppm)

| Sample No. | 29631 | 29632 | 29635 | 29639 | 29645 | 29647 | 29653 | 29655 | 29661 | 29673 | 29679 | 29685 | 29691 |
|---|---|---|---|---|---|---|---|---|---|---|---|---|---|
| Depth (m) | 1-2 | 2-3 | 5-6 | 9-10 | 15-16 | 17-18 | 22-23 | 24-25 | 30-31 | 42-43 | 47-48 | 53-54 | 59-60 |
| $SiO_2$ | 73.6 | 65.6 | 52.8 | 64.2 | 66.5 | 56.4 | 57.6 | 58.4 | 68.5 | 75.5 | 70.7 | 73.6 | 62.3 |
| $Al_2O_3$ | 8.41 | 18.6 | 13.8 | 18.7 | 16.3 | 15.6 | 12.1 | 18.6 | 19.6 | 12.7 | 17.7 | 15.1 | 18.4 |
| $Fe_2O_3$ | 11.4 | 3.94 | 20.5 | 4.19 | 5.76 | 16.8 | 20.8 | 11.4 | 1.51 | 4.40 | 1.88 | 0.58 | 1.08 |
| MgO | 0.22 | 0.42 | 0.39 | 0.42 | 0.44 | 0.31 | 0.23 | 0.32 | 0.28 | 0.16 | 0.24 | 0.32 | 0.59 |
| CaO | 0.22 | 0.15 | <0.04 | 0.06 | <0.04 | <0.04 | <0.04 | <0.04 | <0.04 | <0.04 | <0.04 | <0.04 | 0.69 |
| $Na_2O$ | 0.09 | 0.58 | 1.13 | 1.42 | 1.19 | 0.86 | 0.70 | 1.12 | 0.81 | 0.77 | 0.70 | 1.36 | 2.01 |
| $K_2O$ | 1.51 | 3.08 | 1.78 | 1.66 | 2.81 | 1.95 | 1.55 | 2.25 | 3.02 | 1.15 | 2.26 | 2.00 | 2.48 |
| $TiO_2$ | 0.34 | 0.81 | 0.62 | 0.70 | 0.51 | 0.44 | 0.32 | 0.54 | 0.50 | 0.43 | 0.32 | 0.42 | 0.48 |
| $SO_3$ | 0.18 | 0.49 | 0.62 | 0.14 | 0.94 | 0.44 | 0.10 | 0.15 | 0.05 | 0.05 | <0.03 | 0.13 | 0.32 |
| As | 1100 | 500 | 2500 | 350 | 410 | 1100 | 2200 | 910 | 60 | 160 | 52 | 32 | 58 |
| Au | 0.05 | - | 0.96 | <0.02 | <0.02 | <0.02 | <0.02 | 0.03 | <0.02 | <0.02 | <0.02 | <0.02 | 0.04 |
| B | 40 | 50 | 40 | 60 | 60 | 60 | 50 | 80 | 50 | 40 | 30 | 40 | 80 |
| Ba | 440 | 970 | 650 | 640 | 760 | 520 | 400 | 560 | 700 | 340 | 660 | 700 | 640 |
| Co | 11 | 9 | 12 | 8 | 8 | 9 | 12 | 7 | 7 | 5 | 6 | 6 | 6 |
| Cr | 220 | 350 | 310 | 270 | 300 | 300 | 160 | 450 | 270 | 350 | 110 | 84 | 210 |
| Cu | 75 | 42 | 110 | 17 | 34 | 34 | 23 | 9 | <5 | <5 | 6 | <5 | 11 |
| Ga | 10 | 30 | 20 | 30 | 20 | 20 | 15 | 20 | 20 | 15 | 20 | 10 | 15 |
| Ge | 0.3 | 0.3 | 0.1 | 2 | 0.3 | 1 | 0.5 | 1 | 0.1 | 0.5 | <0.1 | <0.1 | 1 |
| Mo | 2 | 3 | 2 | 3 | 3 | 5 | 3 | 2 | 2 | 3 | 2 | 2 | 3 |
| Ni | 110 | 91 | 140 | 74 | 61 | 120 | 210 | 79 | 70 | 44 | 60 | 57 | 46 |
| Pb | 64 | 71 | 93 | 54 | 61 | 74 | 76 | <50 | <50 | <50 | <50 | <50 | <50 |
| Sc | 11 | 27 | 19 | 16 | 12 | 13 | 12 | 23 | 23 | 21 | 8 | <5 | 14 |
| Sn | <0.3 | 2 | 1 | 2 | 2 | 1 | 1 | 2 | 1 | 1 | 0.5 | 0.5 | 2 |
| Sr | 35 | 64 | 45 | 35 | 81 | 62 | 36 | 53 | 80 | 37 | 70 | 78 | 170 |
| V | 100 | 180 | 170 | 130 | 110 | 120 | 78 | 140 | 98 | 130 | 58 | 55 | 86 |
| W | <10 | 10 | 20 | 50 | 10 | <10 | <10 | <10 | <10 | <10 | <10 | <10 | <10 |
| Y | 8 | 13 | 11 | 11 | 9 | 8 | 7 | 9 | 10 | 7 | 7 | 8 | 10 |
| Zn | 92 | 41 | 200 | 20 | 19 | 79 | 280 | 14 | 7 | <5 | < | <5 | <5 |
| Zr | 81 | 170 | 140 | 180 | 150 | 150 | 100 | 120 | 150 | 100 | 160 | 170 | 180 |
| Ti/Zr | 25 | 28 | 26 | 24 | 20 | 18 | 18 | 26 | 19 | 25 | 12 | 14 | 16 |

Note: $P_2O_5$ ≤0.1, MnO <0.04%; Ag <0.1, Sb < 10 ppm

Table 4. Average compositions of zones PSRC 172 (mineralized) (major elements, wt%; minors, ppm)

| Zone | Goe/al | Hem/goe | Fe-poor | Paragonite |
|---|---|---|---|---|
| Depth (m) | 0-18 | 18-27 | 27-43 | 43-60 |
| No. of samples | 6 | 2 | 2 | 3 |
| $SiO_2$ | 63.2 | 58.0 | 72.0 | 68.9 |
| $Al_2O_3$ | 15.2 | 15.4 | 16.2 | 17.1 |
| $Fe_2O_3$ | 10.4 | 16.1 | 2.96 | 1.18 |
| MgO | 0.37 | 0.28 | 0.22 | 0.38 |
| CaO | 0.08 | <0.04 | <0.04 | 0.24 |
| $Na_2O$ | 0.88 | 0.91 | 0.79 | 1.36 |
| $K_2O$ | 2.13 | 1.70 | 2.09 | 2.25 |
| $TiO_2$ | 0.57 | 0.43 | 0.47 | 0.41 |
| $SO_3$ | 0.47 | 0.13 | 0.05 | 0.16 |
| Ag | <0.1 | <0.1 | <0.1 | <0.1 |
| As | 990 | 1570 | 110 | 47 |
| Au | 0.21 | 0.02 | <0.02 | 0.02 |
| B | 52 | 65 | 45 | 50 |
| Ba | 660 | 480 | 520 | 670 |
| Co | 10 | 10 | 6 | 6 |
| Cr | 290 | 310 | 310 | 130 |
| Cu | 50 | 16 | <5 | 6 |
| Ga | 22 | 18 | 18 | 15 |
| Ge | 0.7 | 0.8 | 0.3 | 0.4 |
| Mo | 3 | 3 | 3 | 2 |
| Ni | 99 | 140 | 57 | 54 |
| Pb | 70 | <50 | <50 | <50 |
| Sc | 16 | 18 | 22 | 8 |
| Sn | 1 | 2 | 1 | 1 |
| Sr | 54 | 45 | 59 | 110 |
| V | 140 | 110 | 110 | 66 |
| W | 17 | <10 | <10 | <10 |
| Y | 10 | 8 | 9 | 8 |
| Zn | 75 | 150 | <5 | <5 |
| Zr | 150 | 110 | 130 | 170 |

Table 5. Compositions of fresh shales, drill holes PSRCD 309 and PSRCD 310
(majors, wt%; minors, ppm)

| Sample hole | 105681 | 108074 | 108075 | 105683 | Average |
|---|---|---|---|---|---|
| Drill hole | 310 | 309 | 309 | 309 | Barren Shale |
| Depth (m) | 154.1 | 217 | 219.5 | 222.1 | |
| | mineralized ← | barren → | | | |
| $SiO_2$ | 68.3 | 60.5 | 56.5 | 43.3 | 53.4 |
| $Al_2O_3$ | 8.11 | 21.7 | 17.1 | 12.5 | 17.1 |
| $Fe_2O_3$ | 8.48 | 1.24 | 4.85 | 2.45 | 2.85 |
| MgO | 1.23 | 1.08 | 1.62 | 5.27 | 2.66 |
| CaO | <0.04 | 0.94 | 3.27 | 13.0 | 5.74 |
| $Na_2O$ | 0.16 | 3.30 | 5.49 | 3.24 | 4.01 |
| $K_2O$ | 1.92 | 5.26 | 1.88 | 1.79 | 2.98 |
| $TiO_2$ | 0.33 | 0.62 | 0.65 | 0.44 | 0.56 |
| MnO | <0.1 | 0.23 | 0.17 | 0.23 | 0.21 |
| S | 5.73 | 0.53 | 1.44 | 0.50 | 0.82 |
| Ag | 2 | 0.3 | 0.3 | 0.2 | 0.3 |
| As | 14 | 13 | 16 | 18 | 16 |
| Au | 0.96 | <0.01 | <0.01 | <0.01 | <0.01 |
| B | 100 | 80 | 40 | 50 | 57 |
| Ba | 310 | 660 | 370 | 370 | 470 |
| Co | 92 | 12 | 25 | 13 | 17 |
| Cr | 70 | 45 | 83 | 50 | 59 |
| Cu | 260 | 45 | 87 | 33 | 55 |
| Ga | 15 | 40 | 30 | 20 | 30 |
| Ge | 3 | 4 | 3 | 3 | 3 |
| Mo | 6 | 2 | 3 | 2 | 2 |
| Ni | 190 | 36 | 48 | 43 | 42 |
| Pb | 88 | 12 | 10 | 10 | 11 |
| Sb | 12 | 1 | 2 | 0.4 | 1 |
| Sc | 21 | 26 | 11 | <5 | 13 |
| Sn | 15 | 6 | 4 | 2 | 4 |
| Sr | 8 | 210 | 360 | 230 | 270 |
| Tl | <3 | 8 | 5 | 4 | 6 |
| V | 56 | 84 | 120 | 70 | 91 |
| W | 6 | <2 | <2 | <2 | <2 |
| Y | 8 | 8 | 10 | 9 | 9 |
| Zn | 90 | 220 | 540 | 200 | 160 |
| Zr | 74 | 210 | 150 | 120 | 160 |
| Ti/Zr | 27 | 16 | 25 | 22 | 21 |

Table 6. Structural formulae (based on 22 O) and trace element contents for white micas, Panglo Shales

| Sample No. | 29635 | 108074 | 105682 | 50371 | 50371 | 50381 | 50381 | 50381 | 50381 | 50420 | 50420 | 50428 |
|---|---|---|---|---|---|---|---|---|---|---|---|---|
| Drill hole | 172 | 309 | 310 | 340 | 340 | 340 | 340 | 340 | 340 | 341 | 341 | 341 |
| Depth (m) | 5-6 | 217 | 173 | 19-20 | 19-20 | 28-29 | 28-29 | 28-29 | 28-29 | 6-7 | 6-7 | 12-13 |
| No.of analyses | 6 | 8 | 7 | 6 | 3 | 2 | 6 | 5 | 3 | 5 | 4 | 5 |
| K | 1.50 | 1.69 | 1.55 | 1.28 | 0.63 | 0.48 | 0.81 | 0.67 | 0.53 | 1.62 | 1.19 | 1.28 |
| Na | 0.13 | 0.11 | 0.14 | 0.37 | 0.76 | 1.04 | 0.71 | 0.70 | 0.37 | 0.13 | 0.11 | 0.35 |
| Ba | 0.01 | 0.01 | 0.01 | 0.01 | 0.01# | 0+ | 0# | 0.01# | 0* | 0 | 0 | 0.01 |
| ΣX | 1.64 | 1.81 | 1.70 | 1.66 | 1.43 | 1.55 | 1.55 | 1.41 | 0.91 | 1.75 | 1.30 | 1.64 |
| Al | 3.75 | 3.61 | 3.49 | 3.88 | 4.03 | 3.98 | 3.93 | 3.83 | 3.66 | 3.79 | 3.95 | 3.70 |
| $Fe^{II}$ | 0.20 | 0.07 | 0.20 | 0.06 | 0.04 | 0.06 | 0.06 | 0.04 | 0.05 | 0.05 | 0.05 | 0.06 |
| Mg | 0.15 | 0.29 | 0.31 | 0.11 | 0.04 | 0.07 | 0.08 | 0.07 | 0.05 | 0.21 | 0.19 | 0.15 |
| Ti | 0.03 | 0.02 | 0.03 | 0.01 | 0.01 | 0.01 | 0.01 | 0 | 0.01 | 0.01 | 0.02 | 0.02 |
| ΣY | 4.13 | 3.99 | 4.03 | 4.06 | 4.12 | 4.12 | 4.08 | 3.94 | 3.77 | 4.08 | 4.21 | 3.93 |
| Si | 6.31 | 6.53 | 6.67 | 6.31 | 6.27 | 6.20 | 6.32 | 6.86 | 7.90 | 6.26 | 6.26 | 6.73 |
| Al | 1.69 | 1.47 | 1.33 | 1.69 | 1.73 | 1.80 | 1.68 | 1.14 | 0.10 | 1.74 | 1.74 | 1.27 |
| OH | 3.97 | 3.92 | 3.92 | 3.89 | 3.92 | 3.88 | 3.88 | 3.80 | 3.94 | 3.98 | 3.90 | 3.84 |
| F | 0.05 | 0.05 | 0.05 | 0.09 | 0.05 | 0.03 | 0.02 | 0.09 | 0.03 | 0.04 | 0.04 | 0.06 |
| Cl | 0.01 | 0.01 | 0.02 | 0.02 | 0.06 | 0.15 | 0.11 | 0.11 | 0.07 | 0 | 0.03 | 0.08 |
| Cr (ppm) | 210 | 100 | 140 | 190 | 210 | 240 | 150 | 240 | 120 | 150 | <100 | <100 |
| Ni (ppm) | <100 | <100 | <100 | <100 | <100 | <100 | <100 | <100 | <100 | <100 | <100 | <100 |
| Cu (ppm) | <100 | 130 | 170 | 110 | 150 | 380 | 230 | 230 | 120 | <100 | 120 | 230 |
| Zn (ppm) | <100 | 100 | 170 | <100 | <100 | <100 | <100 | <100 | <100 | <100 | <100 | <100 |
| Sr (ppm) | <100 | <100 | <100 | 250 | 620 | 550 | 510 | 480 | 250 | <100 | <100 | 160 |
| Ba (ppm) | 2400 | 970 | 1650 | 1660 | 750 | 570 | 700 | 1000 | 530 | <100 | <100 | 820 |
| Fe*% | 57 | 20 | 39 | 35 | 51 | 49 | 46 | 38 | 54 | 20 | 22 | 27 |
| Mineral | Musc | Musc | Musc | Na musc | Bram | Parag | Na musc | Bram | Na Illite | Musc | Illite | Na musc |
| Profile | ←------ Mineralized --→ | | | ←---------------------- Barren ---------------→ | | | | | | ←--- Mineralized ----→ | | |

# Ca = 0.02 Sr = 0.01
+ Ca = 0.03
* Ca = 0.01

Table 7. Minor and trace element contents of chlorite, kaolinite and tourmaline, Panglo shales (ppm)

| Mineral | Sample No. | Drill hole | Depth (m) | Fe* | Cr | Ni | Cu | Zn | Sr | Ba |
|---|---|---|---|---|---|---|---|---|---|---|
| Chlorite | 108074 | PSRCD309 | 217 | 54 | <100 | <100 | <100 | 400 | <100 | <100 |
| | 108074 | PSRCD309 | 217 (vein) | 64 | 100 | <100 | <100 | 300 | <100 | <100 |
| | 105682 | PSRCD310 | 173 | 61 | <100 | 120 | 200 | 670 | <100 | <100 |
| Kaolinite | 29635 | PSRC172 | 5-6 | 93 | 340 | <100 | <10 | <100 | <100 | 500 |
| | 29645 | PSRC172 | 15-16 | 40 | 350 | <100 | <100 | <100 | <100 | 960 |
| | 29655 | PSRC172 | 24-25 | 84 | 120 | <100 | <100 | <100 | <100 | 190 |
| Tourmaline | 29655 | PSRC172 | 24-25 | 37 | 640 | <100 | <100 | 110 | 110 | <100 |

Table 8. Minor and trace element contents in oxide phases, Panglo shales (ppm)

| Mineral | Sample No. | Drill hole | Depth (m) | Cr | Ni | Cu | Zn | As | Sb |
|---|---|---|---|---|---|---|---|---|---|
| Goethite | 29635 | PSRC172 | 5-6 (diss) | 310 | 200 | 950 | 900 | 1.66% | 100 |
| | 29635 | PSRC172 | 5-6 (coll) | 120 | 610 | 190 | 1900 | 1.99% | 150 |
| | 29645 | PSRC172 | 15-16 | 2600 | 120 | 280 | 190 | 1.87% | 180 |
| | 29655 | PSRC172 | 24-25 | 700 | <100 | 130 | 140 | 0.34% | 190 |
| | 50371 | PSRC340 | 19-20 | - | - | - | - | 0.09% | - |
| | 50381 | PSRC340 | 28-29 | <100 | - | - | 160 | 0.42% | - |
| Hematite | 50371 | PSRC340 | 19-20 | - | - | - | - | 0.16% | - |
| | 50381 | PSRC340 | 28-29 | <100 | - | - | <100 | 0.22% | - |
| | 50420 | PSRC341 | 6-7 | - | - | - | - | 0.01% | - |
| Rutile | 29645 | PSRC172 | 15-16 | 1600 | | | | | |
| | 50428 | PSRC341 | 12-13 | 240 | | | | | |
| | 108074 | PSRC309 | 217 | 360 | | | | | |
| Ilmenite | 29645 | PSRC172 | 15-16 | 900 | | | | | |

diss ≡ disseminated    coll ≡ colloform

Table 9. Composition (at%) of carbonates, Panglo shales

| Sample | Drill hole | Depth (m) | | Ca | Mg | Fe | Mn | Sr | Mn/Fe |
|---|---|---|---|---|---|---|---|---|---|
| | | | | atomic % | | | | | |
| Dolomite | | | | | | | | | |
| 108074 | PSRCD309 | 217 | | 50.6 | 45.6 | 3.54 | 0.46 | - | 0.13 |
| 105682 | PSRCD310 | 173 | late stage | 49.9 | 43.6 | 5.52 | 0.96 | 0.02 | 0.18 |
| | | | earlier " | 51.3 | 33.4 | 14.5 | 0.82 | 0.01 | 0.06 |
| Siderite | | | | | | | | | |
| 108074 | PSRCD309 | 217 | | 11.2 | 1.01 | 87.2 | 0.61 | 0 | 0.007 |
| 105682 | PSRCD310 | 173 | | 12.6 | 1.89 | 84.5 | 1.04 | - | 0.012 |

Table 10. Compositions of alunites, Panglo shales (mols, based on 2 mols ($XO_4$))

| Sample No. | 29645 | 50363 | 50420 | 50428 | 50428 |
|---|---|---|---|---|---|
| Drill Hole | 172 | 340 | 341 | 341 | 341 |
| Depth (m) | 15-16 | 11-12 | 6-7 | 12-13 | 12-13 |
| K | 0.63 | 0.66 | 0.79 | 0.72 | 0.61 |
| Na | 0.18 | 0.19 | 0.15 | 0.19 | 0.36 |
| Sr | 0.01 | 0.04 | 0.01 | 0.01 | 0.01 |
| Ca | 0 | 0.02 | 0 | 0.01 | 0.01 |
| Ba | 0.01 | 0.01# | 0 | 0 | 0# |
| Al | 2.89 | 2.93 | 2.91 | 2.55 | 2.82 |
| Fe | 0.05 | 0.06 | 0.05 | 0.30 | 0.03 |
| Cu | 0 | 0.01 | 0.01 | 0.01 | 0.01 |
| $SO_4$ | 1.98 | 1.91 | 1.95 | 1.96 | 1.98 |
| $PO_4$ | 0.01 | 0.09 | 0.04 | 0.04 | 0.02 |
| $AsO_4$ | 0.01 | 0 | 0.01 | 0 | 0 |
| OH (calc) | 5.65 | 5.91 | 5.79 | 5.48 | 5.74 |
| Sr (ppm) | 1400 | 6500 | 1200 | 1900 | 1400 |
| Ba (ppm) | 1100 | 3100 | 500 | 170 | <100 |

Note # 0.01 mol Pb also present

Table 11. Minor element contents of pyrite, Panglo shales (wt%)

| Sample No. | 108074 | 108074 | 108074 | 108074 | 105682 | 105682 | 105682 |
|---|---|---|---|---|---|---|---|
| Drill hole | PSRCD309 | | | | PSRCD310 | | |
| Depth (m) | 217 | | | | 173 | | |
| No. of analyses | 4 | 5 | 6 | 9 | 7 | 6 | 3 |
| As | <0.01 | <0.01 | 0.01 | 0.02 | 0.01 | <0.01 | 0.04 |
| Co | <0.01 | 0.03 | 0.18 | 0.07 | 0.04 | 0.13 | 0.08 |
| Cu | 0.02 | 0.02 | 0.03 | 0.38 | 0.05 | 0.01 | 0.54 |
| Ni | 0.07 | 0.19 | 0.45 | 0.22 | 0.07 | 0.29 | 0.14 |
| Zn | 0.02 | 0.01 | 0.01 | 0.02 | 0.01 | 0.02 | 0.03 |
| Size (μm) | <50 | <100 | <100 | >100 | 10-100 | 5-100 | 10-100 |

Table 12. Average compositions for zones, PSRC342 (mineralized) (major elements, wt %; minors, ppm)

| Zone | Kaolinite | Alunite | Musc/kaol | Musc/kaol (min) |
|---|---|---|---|---|
| Depth (m) | 0-6 | 6-29 | 29-40 | 40-43 |
| No of samples | 3 | 12 | 8 | 3 |
| $SiO_2$ | 42.0 | 68.5 | 64.3 | 67.8 |
| $Al_2O_3$ | 31.0 | 15.2 | 18.2 | 12.5 |
| $Fe_2O_3$ | 9.86 | 6.70 | 6.15 | 6.89 |
| MgO | 0.36 | 0.35 | 0.46 | 0.61 |
| CaO | <0.04 | <0.04 | <0.04 | <0.04 |
| $Na_2O$ | 0.86 | 0.58 | 0.74 | 1.23 |
| $K_2O$ | 3.55 | 2.67 | 3.34 | 2.31 |
| $TiO_2$ | 1.98 | 0.41 | 0.58 | 0.55 |
| $SO_3$ | 0.26 | 0.91 | <0.1 | <0.1 |
| Ag | 0.1 | 0.2 | 1.4 | 9 |
| As | 290 | 200 | 330 | 260 |
| Au | 0.01 | <0.01 | <0.01 | 1.5 |
| Ba | 390 | 310 | 490 | 490 |
| Co | 7 | <5 | 49 | 17 |
| Cr | 330 | 110 | 300 | 99 |
| Cu | 88 | 60 | 190 | 190 |
| Ga | 57 | 22 | 26 | 28 |
| Ge | 2 | 2 | 4 | 5 |
| Mo | 5 | 9 | 8 | 10 |
| Ni | 52 | <20 | 24 | 46 |
| Pb | <50 | <50 | 87 | 74 |
| Sc | 59 | 24 | 28 | 29 |
| Sn | 2 | 3 | 7 | 15 |
| Sr | 36 | 39 | 63 | 53 |
| W | 22 | 18 | 14 | <10 |
| Y | 13 | 5 | 8 | 31 |
| Zn | 130 | 59 | 69 | 97 |
| Zr | 130 | 110 | 120 | 190 |

Note: Data from Scott (1989a) but with XRF-derived As and Ba contents

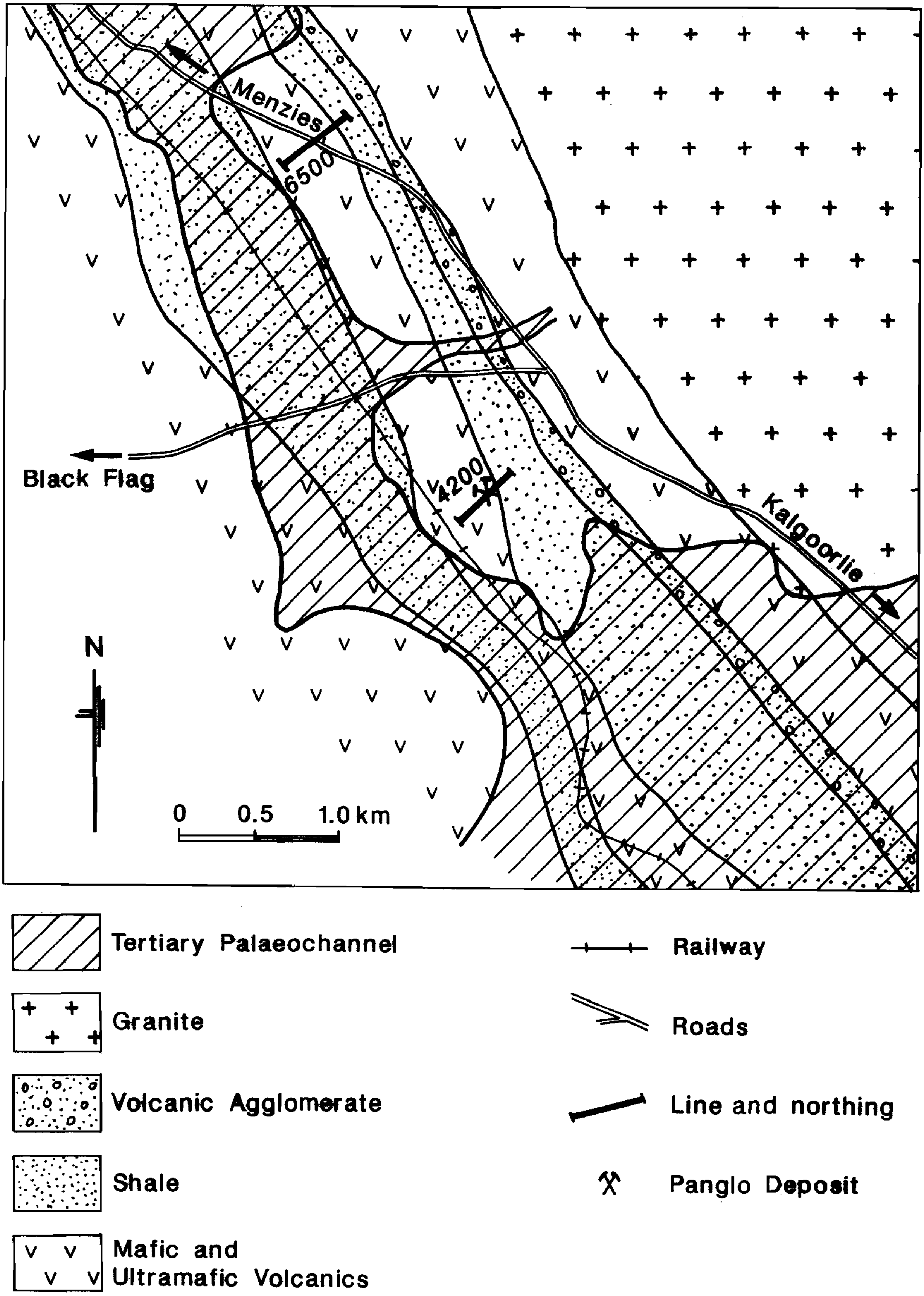


Fig. 1 Geology of the Panglo area, showing the location of Section 6500N relative to 4200N (over the centre of the deposit) (after mapping by Pancontinental Mining Ltd.).

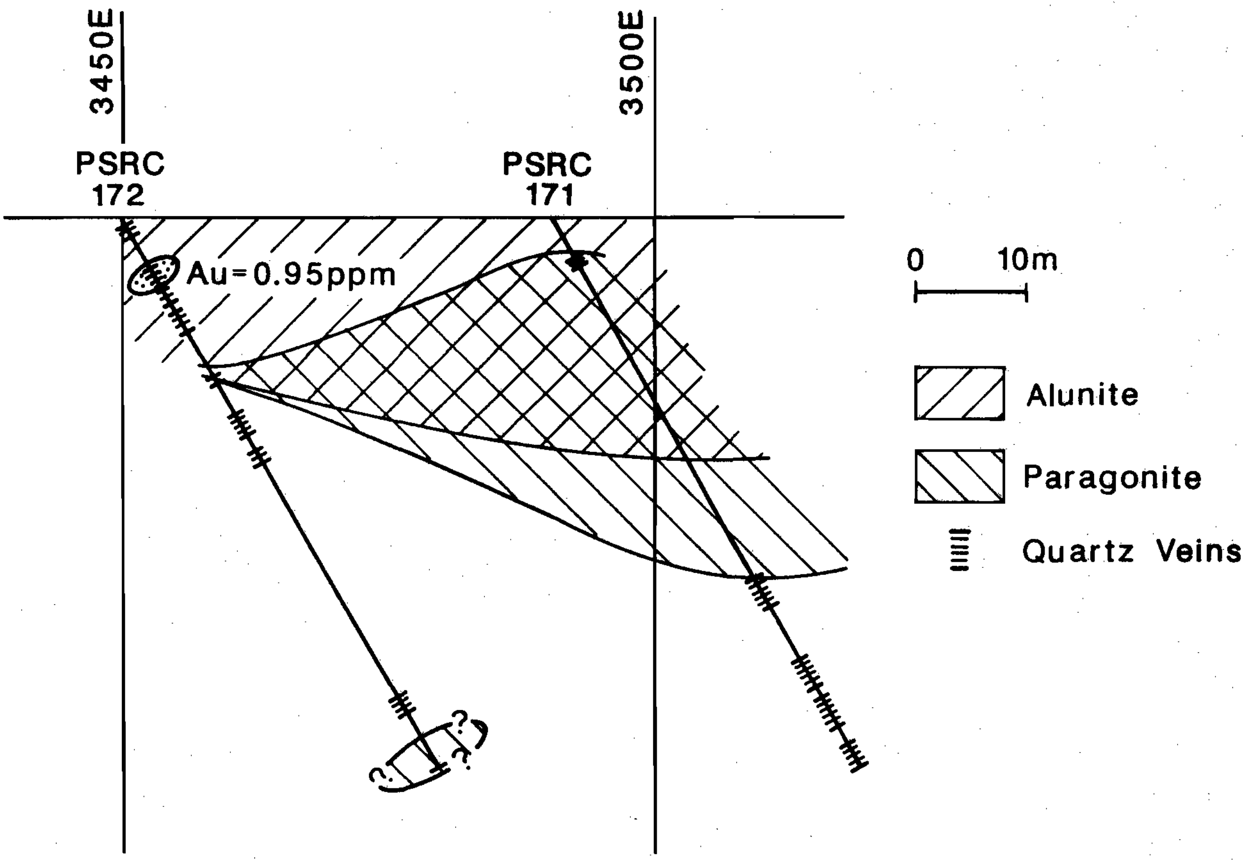


Fig. 2 Section through 6500N, showing features of drill holes PSRC 171 and PSRC 172.

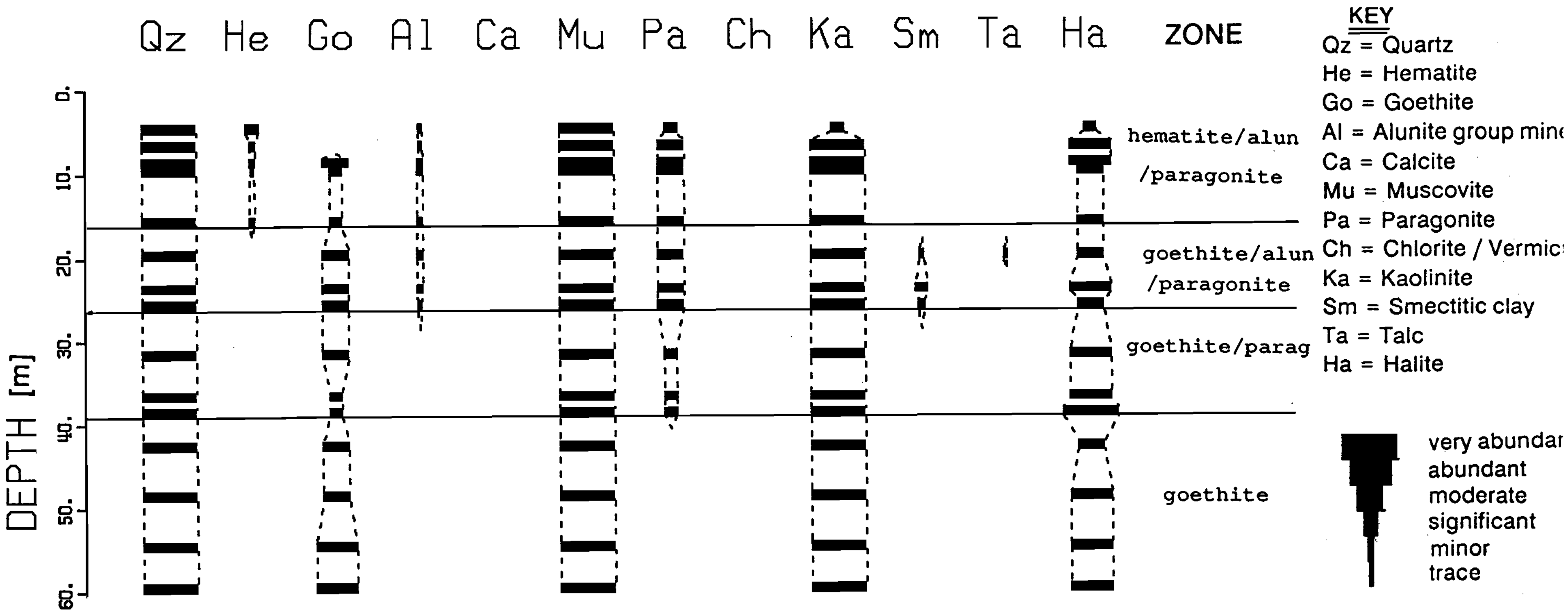


Fig. 3. Mineralogical profile through barren drill hole PSRC 171.

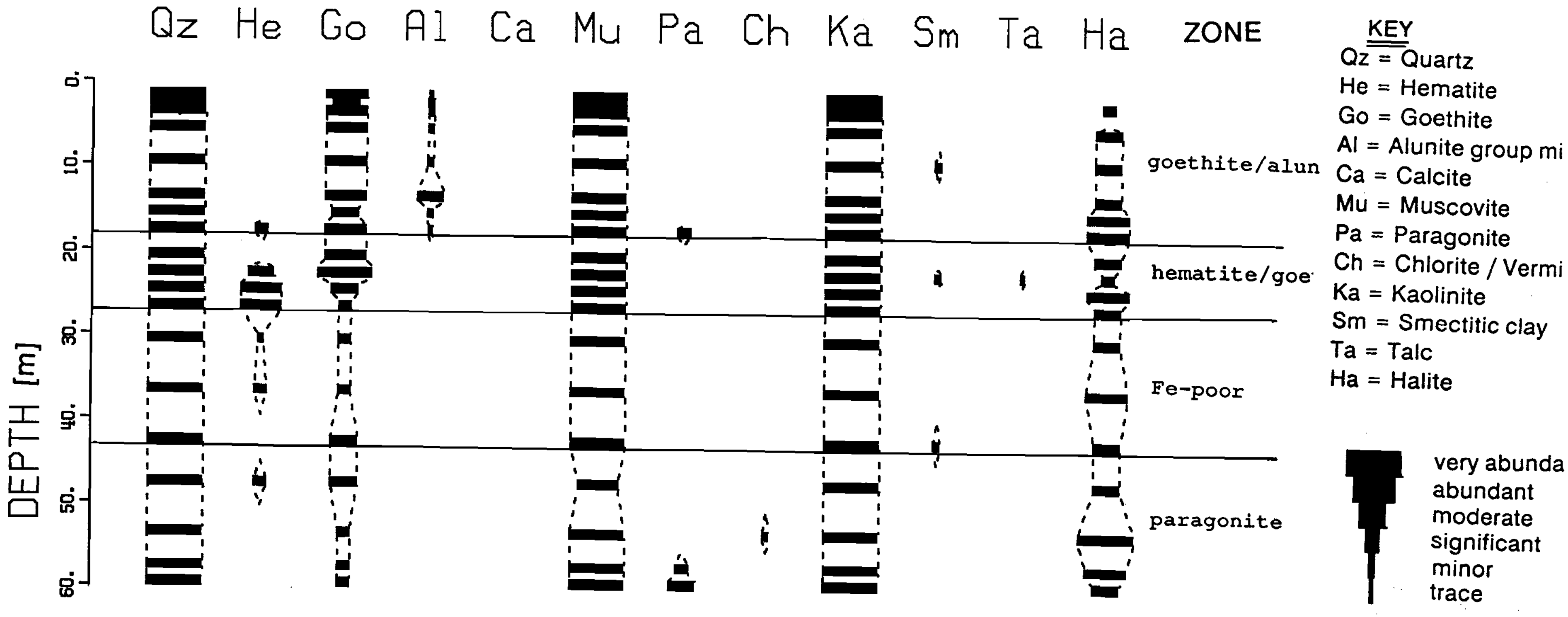


Fig. 4. Mineralogical profile through mineralized drill hole PSRC 172.

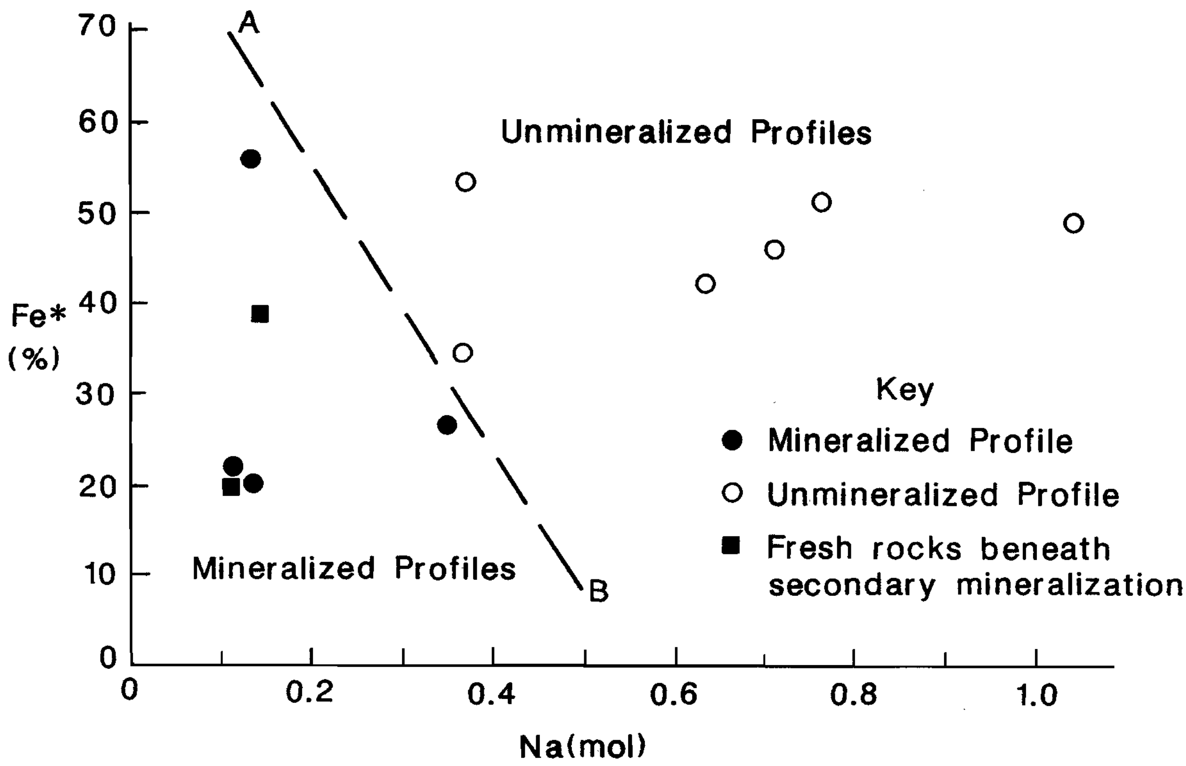


Fig. 5. Fe* vs Na (mols) in white micas in shales, Panglo.

| | Fresh Rock | Saprolite | | | Leached saprolite | | Soil |
|---|---|---|---|---|---|---|---|
| Thickness (m) | | >30 | | | approx 25 | | <1.0 |
| Qtz | ● | ● | ● | ● | ● | ● | ● |
| Plag | | | | | | | ● |
| Calc | | | | | | | ● |
| Dol | ● | | | | | | |
| Alunite | | | | | ● | ● | |
| Hem | | | ● | ● | ● | ● | ● |
| Goe | | ● | ● | ● | ● | ● | ● |
| Magh | | | | | | | ● |
| Musc | ● | ● | ● | ● | ● | ● | ● |
| Parag | | ● | | | | | ● |
| Chl/V | ● | ● | ● | ● | ● | | ● |
| Talc | | | | | | | ● |
| Kaol | | ● | ● | ● | ● | ● | ● |
| Smec | | | ● | ● | ● | ● | ● |
| Pyrite | ● | | | | | | |
| Halite | | ● | ● | ● | ● | ● | |
| Colour | Black to Grey | Grey to Buff | Brown | Brown | Light Brown to Grey | Light Brown | Brown |
| Cr ppm | 70 | 70 | 100 | 300 | 110 | 330 | 380 |
| Au ppm | 1.0 | 0.2 | 1.5 | <0.01 | <0.01 | 0.01 | 0.05 |
| $K_2O$ % | 1.9 | 1.8 | 2.3 | 3.3 | 2.7 | 3.6 | 0.8 |
| $Fe_2O_3$ % | 9 | 3 | 7 | 6 | 7 | 10 | 7 |

Fig. 9. Idealized profile through mineralized shale, Panglo

| | Fresh Rock | Saprolite | | Leached saprolite | | Soil | |
|---|---|---|---|---|---|---|---|
| Thick-ness(m) | | >30 | | approx 25 | | <1.0 | |

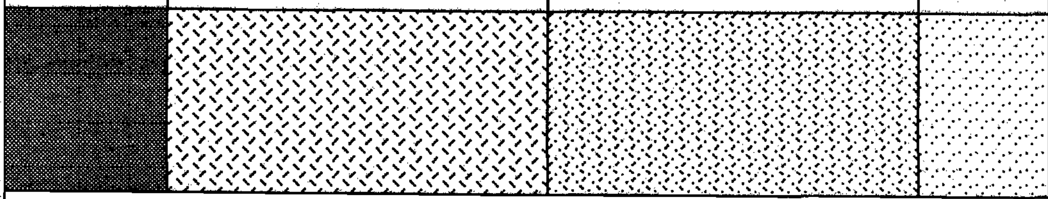

| Fresh Rock | Saprolite | | Leached saprolite | | Soil | |
|---|---|---|---|---|---|---|
| ● | ● | ● | ● | ● | ● | Qtz |
| ● | | | | | ● | Plag |
| ● | | | | | ● | Calc |
| ● | | | | | | Dol |
| | | | ● | ● | | Alunite |
| | | | | ● | ● | Hem |
| | ● | ● | ● | ● | ● | Goe |
| | | | | | ● | Magh |
| ● | ● | ● | ● | ● | ● | Musc |
| | | ● | ● | ● | ● | Parag |
| ● | | | | | ● | Chl/V |
| ● | | | | | ● | Talc |
| | ● | ● | ● | ● | ● | Kaol |
| | | | ● | | ● | Smec |
| ● | | | | | | Pyrite |
| | ● | ● | ● | ● | | Halite |
| Black to Grey | Yellow | White to Grey | White to Pale Brown | White to Pale Brown | Brown | Colour |
| 60 | 130 | 230 | 210 | 230 | 700 | Cr ppm |
| <0.01 | <0.02 | <0.02 | <0.02 | 0.02 | 0.05 | Au ppm |
| 3 | 1.6 | 2.6 | 2.3 | 2.6 | 1.0 | $K_2O$ % |
| 3 | 1.5 | 1.7 | 0.8 | 1.8 | 9 | $Fe_2O_3$% |

Fig. 10. Idealized profile through barren shale, Panglo

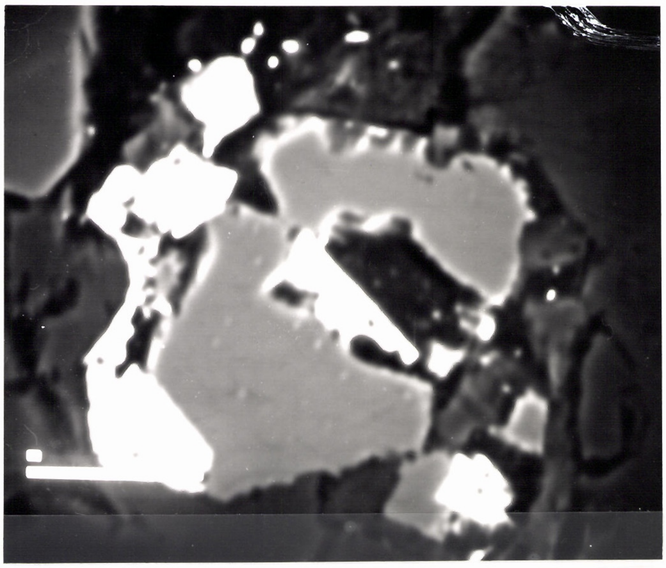

Fig. 6. Siderite (light grey) rimmed by pyrite (white). BSE image, Scale bar = 10 μm (Sample 105682).

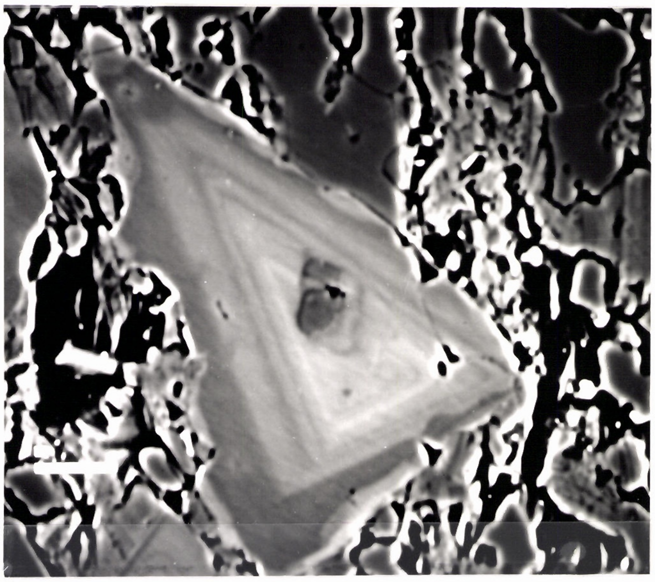

Fig. 7. Zoned dolomite, brighter portions are more Fe rich. BSE image, Scale bar = 10 μm (Sample 105682).

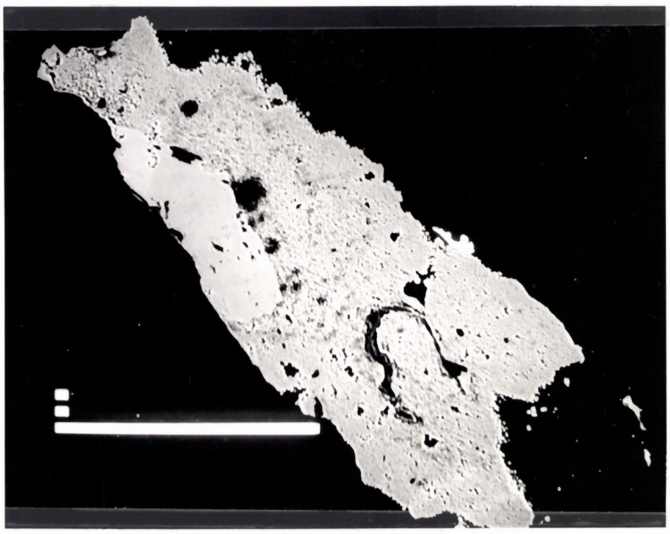

Fig. 8. Porous Cu- and Ni-rich pyrite about brighter Ni-rich pyrite. BSE image, Scale bar = 100 μm (Sample 108074).